

Preparation of AlAsSb and Mid-Infrared (3-5 μ m) Lasers By Metal-Organic Chemical Vapor Deposition

SAND-96-1699C

A. A. Allerman, R. M. Biefeld, and S. R. Kurtz

Sandia National Laboratory, Albuquerque, New Mexico, 87185, USA

CONF-961202-122

ABSTRACT

Mid-infrared (3-5 μ m) infrared lasers and LEDs are being developed for use in chemical sensor systems. As-rich, InAsSb heterostructures display unique electronic properties that are beneficial to the performance of these midwave infrared emitters. We have grown AlAs_{1-x}Sb_x epitaxial layers by metal-organic chemical vapor deposition using trimethylamine (TMAA) or ethyldimethylamine alane (EDMAA), triethylantimony (TESb) and arsine. We examined the growth of AlAs_{1-x}Sb_x using temperatures of 500 to 600 °C, pressures of 70 to 630 torr, V/III ratios of 1-27, and growth rates of 0.3 to 2.7 μ m/hour in a horizontal quartz reactor. The semi-metal properties of a p-GaAsSb/n-InAs heterojunction are utilized as a source for injection of electrons into the active region of lasers. A regrowth technique has been used to fabricate gain-guided lasers using AlAs_{1-x}Sb_x for optical confinement with either a strained InAsSb/InAs multi-quantum well (MQW) or an InAsSb/InAsP strained layer superlattice (SLS) as the active region. Under pulsed injection, the InAsSb/InAs MQW laser operated up to 210K with an emission wavelength of 3.8-3.9 μ m. Under pulsed optical pumping, the InAsSb/InAsP SLS operated to 240K with an emission wavelength of 3.5-3.7 μ m. LED emission has been observed with both active regions in both p-n junction and semi-metal injection structures.

INTRODUCTION

Driven by chemical sensing and infrared countermeasure applications, several mid-infrared (2-6 μ m) diode lasers with strained InAsSb active regions have been recently demonstrated. Devices with AlAsSb claddings have been grown by molecular-beam epitaxy,[1,2] and lasers with higher index, Al free InPSb claddings metal organic chemical vapor deposition (MOCVD) have also been reported.[3] Although AlAsSb claddings provide superior optical confinement, the large conduction band barriers associated with AlAsSb layers can result in poor electron injection and high turn-on voltages. Also, due to lack of satisfactory aluminum sources and residual carbon resulting in p-type doping of AlAsSb alloys, MOCVD growth of AlAsSb injection devices had not been reported. In this paper, we report MOCVD grown lasers with AlAsSb claddings. We describe an electrically injected device which utilizes a GaAsSb(p)/InAs(n) heterojunction to form an internal, semi-metal layer. The semi-metal acts as an internal electron source which can eliminate many of the problems associated with electron injection in these AlAsSb based devices. Furthermore, the use of an internal electron source enables us to consider alternative laser and LED designs that would not be feasible with conventional, p-n junction devices. Initial results for an optically pumped laser with an InAsSb/InAsP strained-layer superlattice (SLS) active region are also presented. Due to a large valence band offset, the light-heavy hole splitting in InAsSb/InAsP SLSs is estimated to be 80 meV, and Auger recombination should be further reduced in this active region.

DISTRIBUTION OF THIS DOCUMENT IS UNLIMITED

MASTER

EXPERIMENT

This work was carried out in a previously described horizontal MOCVD system.[4] TMAA, or EDMAA, TESb, 100% and 10% arsine in hydrogen, and phosphine were the sources for Al, Sb, As and P respectively.

$\text{AlAs}_{0.16}\text{Sb}_{0.84}$ layers 0.5 - 1 μm thick and lattice-matched to InAs were grown over a range of 500 to 600 $^{\circ}\text{C}$ and 76 to 630 torr using a V/III ratio = 1.1 to 27 and a As/V ratio of 0.1 to 0.64 in the gas phase. The growth rate ranged between 0.35 - 2.0 $\mu\text{m}/\text{hr}$. The best morphology was achieved when grown on a buffer layer of InAs or an InAsSb/InAsP strained layer superlattice at a V/III ratio of 7.5 at 500 $^{\circ}\text{C}$ and 200 torr at 1.1 $\mu\text{m}/\text{hr}$.

The two active region structures were used for both laser diode and LED devices. The first consisted of a 10 period multi quantum well (MQW) structure of 85 \AA InSbAs quantum wells with 425 \AA InAs barriers. The other consisted of a 40 period strained layer superlattice (SLS) with the same InSbAs wells but with 85 \AA InAsP barriers.

Secondary ion mass spectroscopy (SIMS) was used to determine C and O impurity concentrations. Five crystal x-ray diffraction (FCXRD) of the (004) reflection was used to determine alloy composition and superlattice period. Layer thickness was determined using a groove technique for thicker layers. Photoluminescence was used to characterize the optical quality of the active regions.

RESULTS AND DISCUSSION

The optimum growth conditions for $\text{AlAs}_x\text{Sb}_{1-x}$ occurred at 500 $^{\circ}\text{C}$ and 200 torr at a growth rate of 1.1 $\mu\text{m}/\text{hour}$ using a V/III ratio of 7.5 assuming a vapor pressure of 0.75 torr for EDMAA at 19.8 $^{\circ}\text{C}$ and an As/V flow ratio of 0.13. Surface morphology was strongly dependent on the InAs substrate. However, the use of a 30 period strain balanced InAsSb/InAsP SLS like that used for the active region greatly improved surface morphology. Surface roughness increased for growth rates of 2 $\mu\text{m}/\text{hr}$. for the same V/III and As/V conditions. Lattice matched GaAsSb cap layers were grown using similar conditions, a V/III of 6.2, and an As/V flow ratio of 0.071. Five crystal x-ray diffraction (FCXRD) measurements of lattice matched AlAsSb films typically exhibited full widths at half of the maximum intensity (FWHM) less than 100 arc seconds. We were also able to reproducibly obtain lattice matching of $\text{AlAs}_x\text{Sb}_{1-x}$ to InAs to within less than 0.015 percent using EDMAA.

The use of other than the above stated growth conditions led to problems in compositional control and reproducibility during the growth of $\text{AlAs}_x\text{Sb}_{1-x}$ layers lattice matched to InAs. Growth at 600 $^{\circ}\text{C}$ resulted in a very broad x-ray peak that extended over hundreds of arc seconds with a constant intensity. Analysis of the x-ray spectra indicated that the large peak width was due to a variation of Sb composition that occurred in the layer as it was grown. Broad x-ray peaks were also observed in films grown using TMAA. The transport of TMAA from the solid source varied during the growth run and changed the V/III ratio resulting in x-ray peaks several hundred arc seconds wide. Sb was also detected by x-ray diffraction in InAs layers grown at 600 $^{\circ}\text{C}$ following previous growths of AlAsSb. We suspect that evaporation of elemental Sb, which has a vapor pressure of 0.1 torr at 600 $^{\circ}\text{C}$, from deposits on the chamber wall results in the compositional drift observed in the AlAsSb layers grown at 600 $^{\circ}\text{C}$. Growth at 500 $^{\circ}\text{C}$ greatly reduces this effect as x-ray peaks with FWHM of less than 100 arc seconds were routinely achieved. Likewise Sb was not detected by x-ray diffraction in InAs layers grown on top of AlAsSb. Growth at 70 or 500 torr yielded broader x-ray diffraction peaks (FWHM 300 arc seconds) with less reproducible lattice matching.

SIMS analysis of undoped AlAsSb showed the oxygen level to be $1.2 \times 10^{19} \text{ cm}^{-3}$ for a film grown at 500 °C and 200 torr using EDMAA. A similar level of oxygen ($1.6 \times 10^{19} \text{ cm}^{-3}$) was found in a film grown at 600 °C and 200 torr using TMAA. The level of carbon found in the film grown at 600 °C was $7.3 \times 10^{17} \text{ cm}^{-3}$ and was much lower than the $2.6 \times 10^{18} \text{ cm}^{-3}$ found in the sample grown at 500 °C. The source of the oxygen found in these materials is unknown at this time. The oxygen could be coming from contaminants in the organometallic sources, the background O in the MOCVD reactor, or from reaction of the samples with air.

The details of the growth of the InAsSb/InAs multiple quantum well (MQW) structures on InAs have been previously published.[5] An x-ray diffraction pattern of an InAs/InAs_{0.89}Sb_{0.11} MQW grown on InAs had sharp satellite peaks out to n=7 indicating good crystalline structure. The structure was grown at 500 °C, 200 torr, a V/III ratio of 25 with an As/V ratio of 0.75 and a growth rate of 2.5 Å/second. A 15 second purge time with reactants switched out of the chamber was used between each layer. The composition, X, of the InAs_{1-x}Sb_x quantum wells could be varied between X = 0.1 and 0.2 by changing the As/V ratio between 0.81 and 0.63 using these growth conditions. The composition changes can be explained by the use of a thermodynamic model as previously discussed.[5]

InAsP layers were grown using 10% AsH₃ in hydrogen with of V/III ratio of 216 and a As/V ratio of .016. The high V/III and low As/V ratios reflect the low thermal decomposition efficiency of PH₃ at 500 °C and 200 torr. The growth rate was 2.5 Å/sec. in the active region.

Low temperature (< 20 K) photoluminescence emission could be controlled between 3.9 to 6.0 μm for Sb compositions between 0.11 to 0.20 in the InAsSb/InAs MQW structures grown on InAs. The long wavelength deviation of these bandgap values from those previously published may be explained by the CuPt-type ordering and phase separation found in these materials.[6, 7] Previous work has shown that the InAs/InAsSb interface band offset in these MOCVD grown materials is type I.[8] PL emission from InAsSb/InAsP SLS structures were blue shifted due to the added confinement provided by the InAsP barriers (Figure 1). PL emission was observed between 3.1 to 4.2 μm for the 20 period SLS shown in Figure 1.

FCXRD of a 20 period InAsSb/InAsP SLS shows sharp SL peaks indicating good structural quality. The n=0 peak is within 10 arc seconds of the substrate indicating the structure is strain balanced. PL emission for the structure grown on InAs is observed at 3.61 μm at 16 K and red shifts to 4.15 μm at 300 K with 8% of the peak intensity at 16 K.

Although the independent growth of the AlAs_xSb_{1-x} layers or the MQW structures gave uniform and reproducible x-ray diffraction patterns, only a very broad x-ray diffraction pattern was observed when the MQW was grown sequentially on top of the AlAs_xSb_{1-x}. When a layer of InAs was grown after a layer of lattice matched AlAs_xSb_{1-x}, a broad x-ray peak was observed at two theta values greater than the InAs substrate. SIMS measurements indicated the presence of Al in the InAs layer. In order to avoid the incorporation of Al into the quantum well structures, we developed a regrowth technique. Following the growth of the 2.5 μm AlAs_xSb_{1-x} confinement layer capped with 500 Å of GaAs_{1-x}Sb_x and a 400 Å layer of InAsSb, the quartz reaction chamber was cleaned before growing the rest of the laser structure. The second growth starts with the active region followed by a second 2.5 μm confinement layer of AlAs_xSb_{1-x} followed by a 1200 Å contact layer of GaAsSb.

None of the layers in the laser structure were intentional doped. The semi-metal nature of the p-GaAsSb / n-InAs interface grown at the end of the first growth is used to inject electrons into the active region. The satellite peaks observed in the first growth are from the InAsSb/InAsP SLS used as a buffer to improve surface morphology (Figure 3). The same structure used in the active region was also used for the buffer. The cladding layer is closely lattice-matched to the substrate.

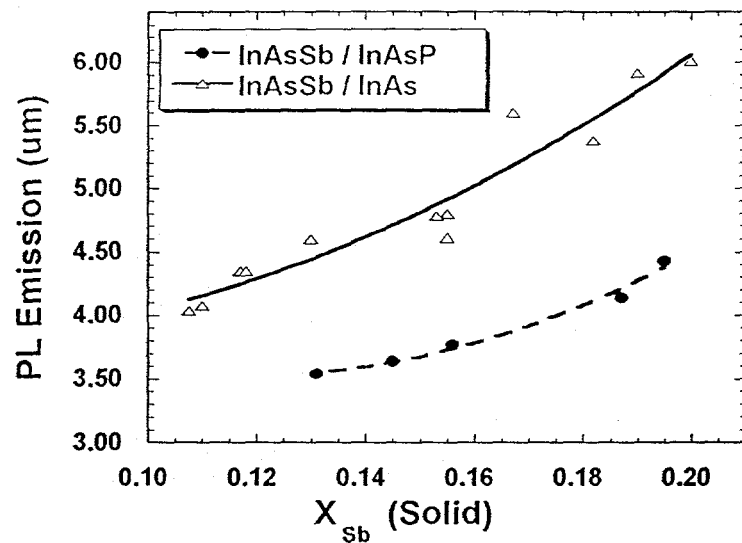


Figure 1. Low temperature photoluminescence ($< 20\text{K}$) from 10 period 85\AA $\text{InSb}_x\text{As}_{1-x}$ / 425\AA InAs MQW's and 40 period 75\AA $\text{InSb}_x\text{As}_{1-x}$ / 84\AA $\text{InAs}_{.76}\text{P}_{.24}$ SLS's grown on InAs.

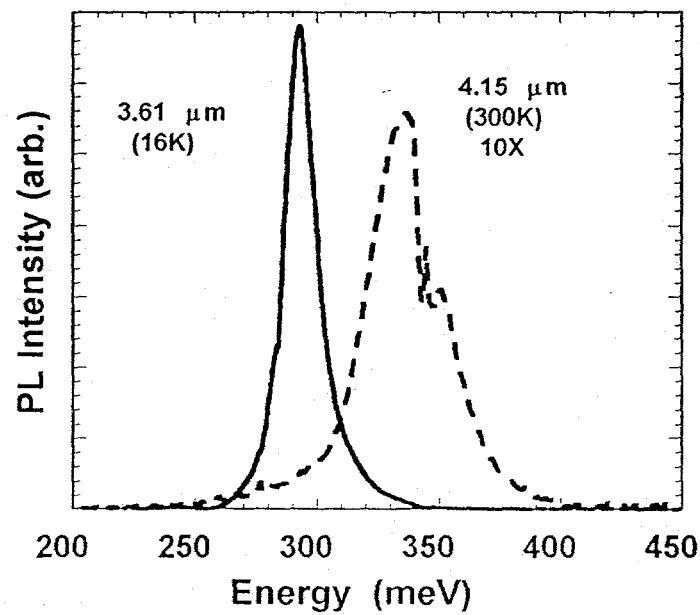


Figure 2. Low temperature photoluminescence from a 40 period 83\AA $\text{InSb}_{.87}\text{As}_{.13}$ / 82\AA $\text{InAs}_{.73}\text{P}_{.27}$ SLS's grown on InAs. The absorption at 350 meV is an artifact in the PL system.

Gain-guided, stripe lasers with a InAsSb/InAs MQW active region and semi-metal electron injection were fabricated. Under pulsed operation with uncoated facets, lasing was observed in forward bias with 40x1000 or 80x1000 micron stripes. No emission occurred under reverse bias. Devices were tested with 100 nsec pulse widths at 10 kHz (0.1 % duty-cycle). Several longitudinal modes were observed in the 3.8-3.9 μ m range. The lasers displayed a sharp threshold current characteristic, and lasing was observed through 210K. Under pulsed operation, peak power levels of 1 mW/facet could be obtained. A characteristic temperature (T_c) in the 30-40 K range was observed, with the lower value (30 K) being misleading due to degradation of the device at higher temperatures. These maximum operating temperature and characteristic temperature values are comparable to the highest values reported to date, for injection lasers of this wavelength with either strained InAsSb or InAs/GaInSb active regions [1,2,9,10]. Unlike bipolar lasers, cw operation of the unipolar laser has not yet been observed.

Lasing emission was also observed from optically pumped structures with InAsSb/InAsP SLS active regions. Several longitudinal modes were observed in the 3.5- 3.7 μ m range and lasing was observed to 240K. The temperature dependence of the threshold had a characteristic temperature (T_c) of 32 K.

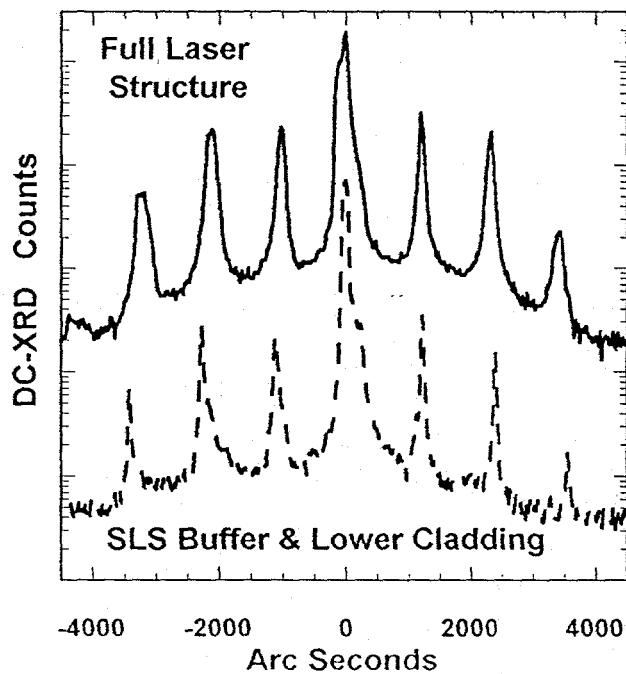


Figure 3. X-ray diffraction pattern of the lower cladding and complete structure following regrowth of the active region and top cladding. An InAsSb / InAsP strain balanced superlattice is used as a buffer to improve surface morphology and as the active region.

LED and laser emission is observed for a variety of forward bias conditions. No emission is observed in reverse bias. The onset of the LED emission coincides with the energy of the InAsSb quantum well photoluminescence. Room temperature LED emission has been observed at 4 μm in excess of 1 μW peak power (10 kHz, 50% duty-cycle). Similar performance has been recorded for LED devices using an InAsSb/InAsP SLS active region. LED emission has been observed from both semi-metal injection and p-n junction structures.

CONCLUSIONS

We have grown $\text{AlAs}_x\text{Sb}_{1-x}$ epitaxial layers by metal-organic chemical vapor deposition (MOCVD) using trimethylamine alane or ethyldimethylamine alane, triethylantimony, and arsine. The growth of high quality $\text{AlAs}_x\text{Sb}_{1-x}$ by MOCVD has been demonstrated and used for optical confinement layers in a 3.8-3.9 μm injection laser with a novel GaSb/InAs semi-metal electron injector. The use of the InAs/GaSb semi-metal for carrier injection, and the compatibility of the semi-metal with InAsSb devices is unique. Diode lasers employing InAsSb/InAs MQW active regions have operated under electrical injection (pulsed) to 210K. Optically pumped laser structures employing strain balanced InAsSb/InAsP SLS active regions have operated to 240K under pulsed conditions.

ACKNOWLEDGEMENTS

We wish to thank J. A. Bur and J. H. Burkhardt who provided technical assistance. This work was performed at Sandia National Laboratories, supported by the U. S. Department of Energy under contract No. DE-AC04-94AL85000

REFERENCES

- [1] H. K. Choi and G. W. Turner, *Appl. Phys. Lett.* **67**, 332 (1995).
- [2] Y-H. Zhang, *Appl. Phys. Lett.* **66**, 118 (1995).
- [3] S. R. Kurtz, R. M. Biefeld, A. A. Allerman, A. J. Howard, M. H. Crawford, and M. W. Pelczynski, *Appl. Phys. Lett.* **68**, 1332 (1996).
- [4] R.M.Biefeld, C.R. Hills, and S.R. Lee, *J. Crys. Growth* **91**, 515 (1988).
- [5] R. M. Biefeld, K. C. Baucom, and S. R. Kurtz, *J. Crystal Growth*, **137**, 231 (1994).
- [6] D. M. Follstaedt, R. M. Biefeld, S. R. Kurtz, and K. C. Baucom, *J. Electronic Mater.* **24**, 819 (1995).
- [7] S. R. Kurtz, L. R. Dawson, R. M. Biefeld, D. M. Follstaedt, and B. L. Doyle, *Phys. Rev. B*, **46**, 1909 (1992).
- [8] S. R. Kurtz, R. M. Biefeld, and A. J. Howard, *Appl. Phys. Lett.*, **67**, 3331 (1995).
- [9] A. A. Allerman, R. M. Biefeld, and S. R. Kurtz, *Appl. Phys. Lett.*, **69**, 465 (1996).
- [10] R. H. Miles (private communication).

DISCLAIMER

This report was prepared as an account of work sponsored by an agency of the United States Government. Neither the United States Government nor any agency thereof, nor any of their employees, make any warranty, express or implied, or assumes any legal liability or responsibility for the accuracy, completeness, or usefulness of any information, apparatus, product, or process disclosed, or represents that its use would not infringe privately owned rights. Reference herein to any specific commercial product, process, or service by trade name, trademark, manufacturer, or otherwise does not necessarily constitute or imply its endorsement, recommendation, or favoring by the United States Government or any agency thereof. The views and opinions of authors expressed herein do not necessarily state or reflect those of the United States Government or any agency thereof.

DISCLAIMER

**Portions of this document may be illegible
in electronic image products. Images are
produced from the best available original
document.**